

## Preparation and Characterization of $Y_2O_3$ Buffer Layers and YBCO Films on Textured Ni Tape

Ataru Ichinose<sup>1</sup>, George Daniels, Chau-Yun Yang and David C. Larbalestier  
Applied Superconductivity Center, University of Wisconsin, Madison, Wisconsin 53706, USA.

Akihiro Kikuchi

Energy Conversion Material Research Group, National Research Institute for Metals, Tsukuba, Ibaraki 305-0047, Japan

Kyoji Tachikawa

Faculty of Engineering, Tokai University, Hiratsuka, Kanagawa 259-1292, Japan

Shirabe Akita

Komae Research Laboratory, Central Research Institute of Electric Power Industry, Komae, Tokyo 201-8511, Japan

**Abstract**— The direct deposition of  $Y_2O_3$  buffer layers on cube-textured nickel tape was successfully performed by electron beam deposition using Y metal which oxidized during deposition. The  $Y_2O_3$  layer exhibited excellent out-of-plane alignment of FWHM of  $2.3 \sim 4^\circ$  and good in-plane alignment with  $\sim 11^\circ$  FWHM. Surface morphology, crystal orientation and grain size proved to be quite sensitive to the deposition pressure. The surface roughness and the grain size increased with increasing deposition pressure, and the crystal orientation changed from  $(111)Y_2O_3$  to  $(100)Y_2O_3$ . Subsequently, YBCO superconducting films were deposited on  $(100)Y_2O_3$  buffer layers by co-evaporation deposition and pulsed-laser deposition (PLD). Though a good in-plane alignment, as measured by X-ray  $\phi$ -scan, was achieved in the YBCO films, their superconducting characteristics were not so good. The  $T_c$  onset was about 84 K for the  $(001)YBCO$  by PLD. The crystal alignment and the microstructure of YBCO superconducting films deposited by the two deposition techniques on cube-textured Ni tapes with  $Y_2O_3$  buffer layers are compared.

facilitated the production of the substrate for YBCO films by recrystallization of cold-rolled pure Ni tape by high temperature vacuum annealing.[5] Biaxially-aligned oxide buffer layers, for example, YSZ/CeO<sub>2</sub>, can be deposited on the RABiTS Ni tape by several kinds of deposition, such as PLD, sputtering and e-beam deposition. YBCO films deposited on both types of metal tapes have  $J_c$  exceeding  $10^6$  A/cm<sup>2</sup> at 77 K in zero field. Their field dependence is reported to be very similar to films made on SrTiO<sub>3</sub> single crystals.

We successfully deposited biaxially-aligned  $Y_2O_3$  buffer layers on cube-textured Ni substrates by electron beam deposition. This technique easily produces the  $Y_2O_3$  buffer layers, needing only control of the deposition pressure. Subsequently, we also deposited YBCO films by co-evaporation deposition and PLD. In this paper, we describe the crystallinity of the  $Y_2O_3$  buffer layers and the YBCO films deposited by these two deposition techniques. The superconducting properties of the YBCO films were briefly investigated.

### I. INTRODUCTION

The fabrication of YBCO superconducting films on metal tapes is focused on the development of long and flexible conductors because of their potential for high critical current density of  $\sim 10^6$  A/cm<sup>2</sup> at 77 K. A most important issue is to decrease the density of high angle crystal boundaries. A crystal boundary with misorientation angle greater than  $\sim 10^\circ$  behaves like a weak-link and the  $J_c$  across such a grain boundary decreases significantly[1], [2]. In order to control the in-plane alignment of polycrystalline YBCO films, several techniques have been developed. Biaxially-aligned yttria-stabilized zirconia (YSZ) buffer layers have been grown on polycrystalline Ni-based alloy tapes by ion-beam-assisted deposition (IBAD) [3], [4]. A process called RABiTS has

Manuscript received Sept. 14, 1998.

This work benefited from EPRI, ORNL and NSF-MRSEC supported facilities.

<sup>1</sup>Permanent address: Central Research Institute of Electric Power Industry

### II. EXPERIMENT

The Ni metal substrates were prepared by rolling of Ni (99.7%) at room temperature followed by recrystallization annealing at  $10^{-6}$  Torr at temperatures between 600 and 900 °C for several hours. The detailed preparation of the substrates has been reported elsewhere[6]. The Ni substrates were shown to have a cube-texture with  $\{001\}\langle 100 \rangle$  orientation. The full-width at half maximum (FWHM) of the out-of-plane and in-plane grain distributions were typically  $\sim 6^\circ$  and  $\sim 12^\circ$ , respectively. These results are shown in Fig. 1.

$Y_2O_3$  buffer layers were deposited by electron beam deposition using an Y metal evaporation source. The deposition temperature, which was measured on the heater side of the substrate mounting block, was 940 °C. Deposition of  $Y_2O_3$  was conducted in both air ( $\sim 10^{-5}$  Torr) and  $N_2$  ( $5 \times 10^{-4}$  Torr) atmosphere. In the deposition of  $Y_2O_3$  buffer layers at  $5 \times 10^{-4}$  Torr  $N_2$  atmosphere, first we pumped down to  $10^{-5}$  Torr air, before introducing  $N_2$  gas into the chamber to control the pressure. We have already reported the  $Y_2O_3$  crystal

alignment dependence of the deposition pressure[6]. It is easy to achieve the (100)Y<sub>2</sub>O<sub>3</sub> oriented film at a higher deposition pressure; however, the Ni is then easily oxidized. Consequently, N<sub>2</sub> gas was used to deposit at high pressure and low oxygen partial pressure.

YBCO films were deposited by both co-evaporation and PLD. In the case of co-evaporation, the temperature was 850 °C measured at the heater side of holder, similar to the case of a Y<sub>2</sub>O<sub>3</sub> deposition. During deposition, pure oxygen gas was introduced near the substrate. After deposition, the films were annealed in 100 Torr of oxygen at T=500 °C. In the case of PLD, the deposition temperature was measured at the surface of the substrate using a pyrometer. The films were deposited at a temperature between 700 and 780 °C at 210

mTorr of O<sub>2</sub> atmosphere and then similarly annealed at ~500 °C for 30 minutes.

The crystal orientation distributions for both YBCO and Y<sub>2</sub>O<sub>3</sub> were evaluated by X-ray diffraction,  $\theta$ - $2\theta$ ,  $\omega$ -scan and  $\phi$ -scan. The surface morphology was observed by scanning electron microscopy (SEM). We measured the J<sub>c</sub> at zero field on bridges which were 200  $\mu$ m wide and 0.5 mm long patterned by photolithography.

### III. RESULTS AND DISCUSSION

Fig. 1 shows the X-ray rocking curves and  $\phi$  scans showing the out-of-plane and in-plane alignment for Y<sub>2</sub>O<sub>3</sub> buffer layers deposited at  $\sim 10^{-5}$  Torr air and  $5 \times 10^{-4}$  Torr N<sub>2</sub>, and the Ni

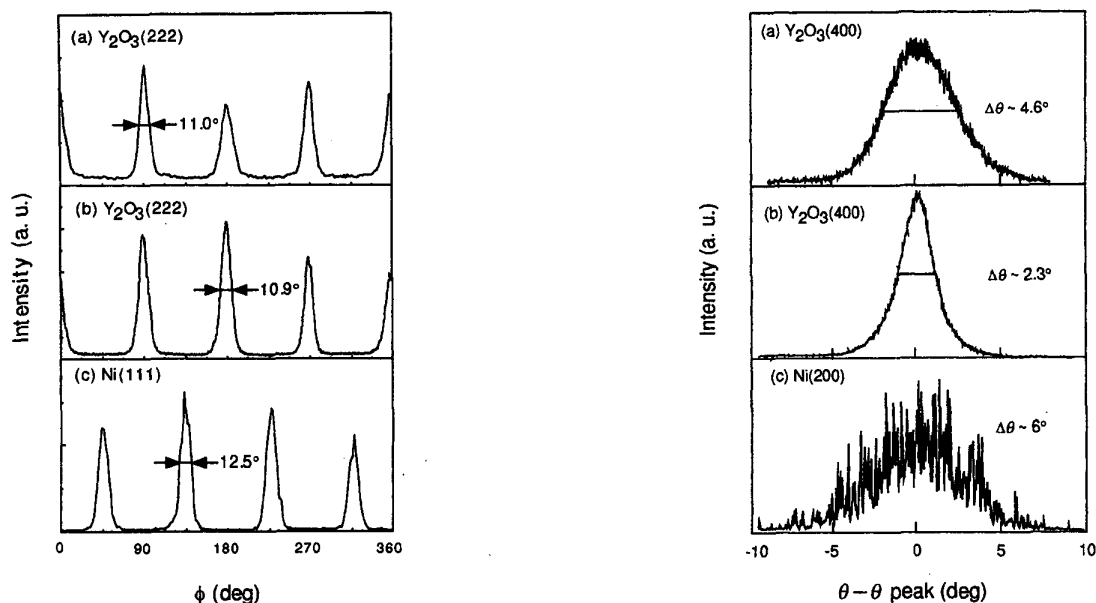
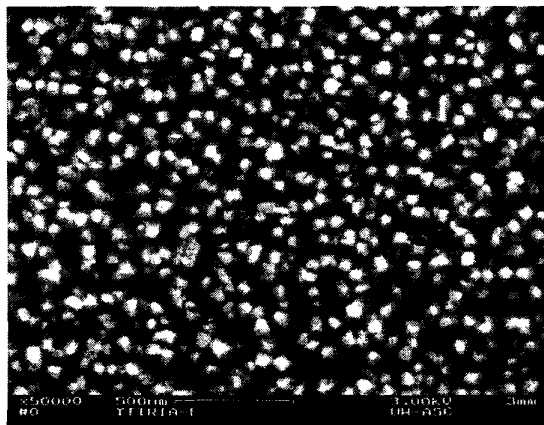


Fig. 1. XRD  $\phi$ -scans (left) and rocking curves (right) showing the out-of-plane and in-plane FWHM for a Y<sub>2</sub>O<sub>3</sub> buffer layer deposited at (a)  $5 \times 10^{-4}$  Torr N<sub>2</sub> and (b)  $\sim 10^{-5}$  Torr air. The Ni substrate scans appear in (c).

(a)



(b)

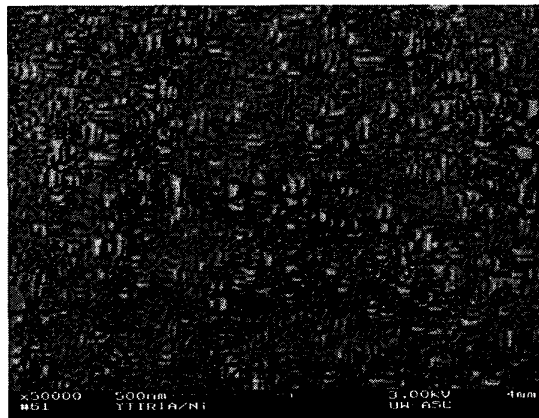


Fig. 2. SEM micrographs for Y<sub>2</sub>O<sub>3</sub> films which were deposited at 940°C at (a)  $5 \times 10^{-4}$  Torr N<sub>2</sub> and (b)  $\sim 10^{-5}$  Torr air.

substrate. The out-of-plane (FWHM  $2.4\text{--}4^\circ$ ) for the  $\text{Y}_2\text{O}_3$  buffer layer is much smaller than the  $\sim 6^\circ$  FWHM for Ni, indicating an improvement in the crystal orientation of the buffer layers. By contrast, the in-plane FWHM for  $\text{Y}_2\text{O}_3$  and Ni are similar at about  $11\text{--}12^\circ$ , indicating good epitaxial growth of  $\text{Y}_2\text{O}_3$  on Ni. Both  $\text{Y}_2\text{O}_3$  buffer layers indicate good biaxial alignment. The SEM images of these films deposited at  $5 \times 10^{-4}$  Torr  $\text{N}_2$  and  $\sim 10^{-5}$  Torr air are shown in Fig. 2(a) and (b), respectively. The grain size and the surface roughness of the buffer layer grown in  $\text{N}_2$  are much greater than for  $\text{Y}_2\text{O}_3$  grown at  $10^{-5}$  Torr. The difference is a result of the different deposition pressure used during growth. The grain size and surface roughness of  $\text{Y}_2\text{O}_3$  increase with increasing deposition pressure[6].

In YBCO films deposited by co-evaporation, regardless of temperature, the formation of (001)YBCO was observed on the  $\text{Y}_2\text{O}_3$  buffer layer deposited at  $\sim 10^{-5}$  Torr air, but (103)YBCO grew on the  $\text{Y}_2\text{O}_3$  buffer layer deposited under  $5 \times 10^{-4}$  Torr  $\text{N}_2$ . Our (001)YBCO films have in-plane alignment of  $11^\circ$  FWHM

according to the (103)YBCO pole figure shown in Fig. 3(a). This indicates that the (001)YBCO film grows epitaxially on the  $\text{Y}_2\text{O}_3$  buffer layer.

In YBCO deposited by PLD, (001)YBCO was observed to form on the  $\text{Y}_2\text{O}_3$  buffer layer deposited at  $\sim 10^{-5}$  Torr air. An in-plane alignment of  $10^\circ$  FWHM was obtained. The (103)YBCO pole figure is shown in Fig. 3(b). In the case of the  $\text{Y}_2\text{O}_3$  buffer layer deposited at  $5 \times 10^{-4}$  Torr  $\text{N}_2$ , YBCO films deposited at  $730^\circ\text{C}$  and  $760^\circ\text{C}$  have predominantly an a-axis and a (103) orientation, respectively.

We also observed the surface morphology of both (100) and (001) YBCO films by SEM. These results are shown in Fig. 4(a), (b), respectively. The surface morphology of both films is very smooth. The grain shape for the (100)YBCO film is rather rectangular with strong grain alignment. The shorter length of the rectangular grains is about  $0.1\ \mu\text{m}$ , slightly larger than the  $\text{Y}_2\text{O}_3$  grain size shown in Fig. 2(a). The (103) oriented grains also have a similar size. On (001)YBCO film, growth islands with well-defined terraces were observed by high

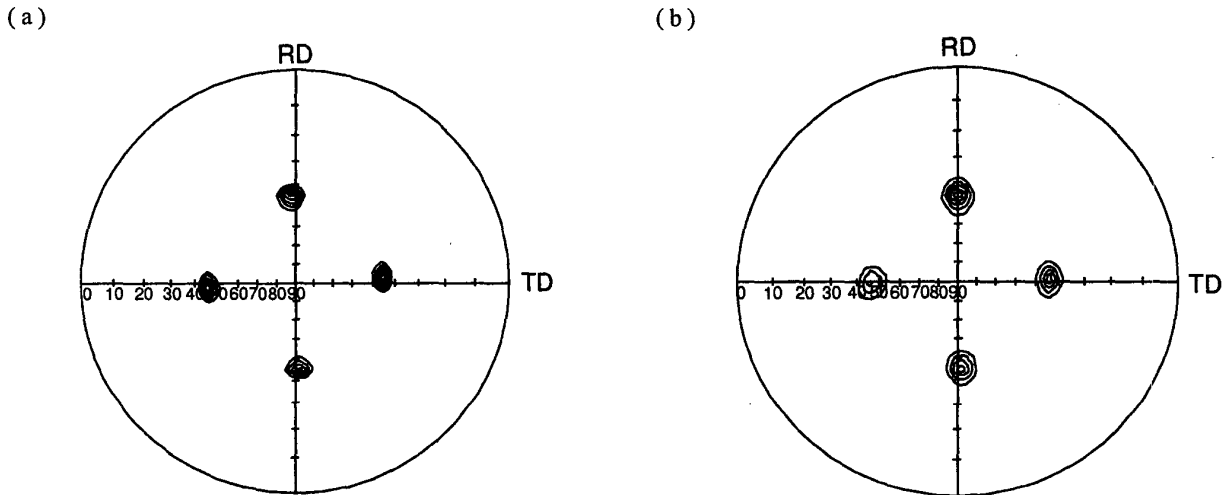


Fig. 3. (103)YBCO pole figures of films deposited by (a) co-evaporation and (b) PLD.

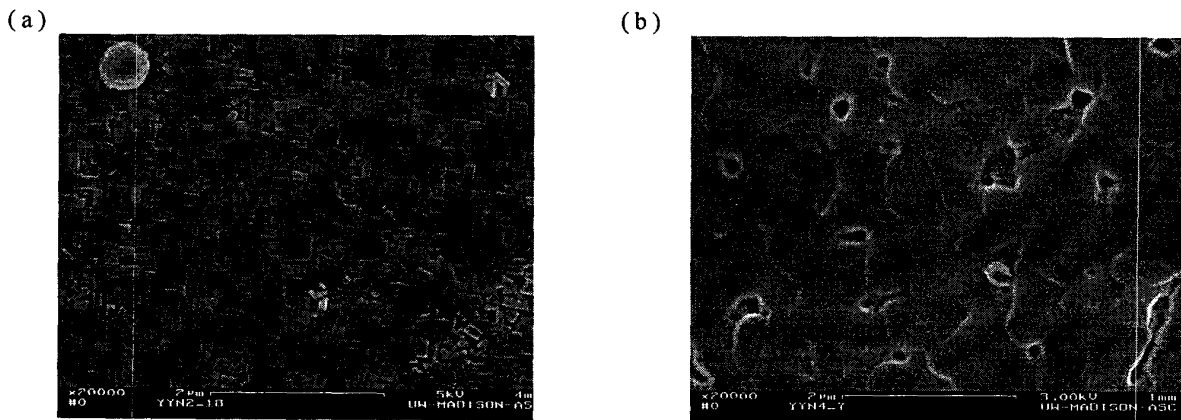


Fig. 4. SEM micrographs of PLD YBCO films on  $\text{Y}_2\text{O}_3$  buffer layers deposited at pressures of (a)  $5 \times 10^{-4}$  Torr  $\text{N}_2$  and (b)  $\sim 10^{-5}$  Torr air.

resolution SEM as shown in Fig. 4(b). The size of the islands ranged from 300 to 600 nm in mean diameter. The grain-to-grain connectivity does appear to be good.

We measured the temperature dependence of the electrical resistance of PLD (001)YBCO films between room temperature and 77 K. The  $T_c$  onset was about 84 K, indicating that the deposition conditions of the YBCO films have not yet been optimized. The  $J_c$  of this sample was  $<10^5$  A/cm<sup>2</sup> at 77 K, probably because of the low  $T_c$ .

#### IV. SUMMARY

We prepared  $Y_2O_3$  buffer layers on cube-textured Ni under two different deposition pressures,  $\sim 10^{-5}$  Torr air and  $5 \times 10^{-4}$  Torr  $N_2$ . Though both buffers possessed good biaxial alignment, their surface morphologies were very different. The  $Y_2O_3$  buffer layer deposited at a higher deposition pressure had a larger grain size and a rougher surface than that deposited at a lower deposition pressure. The out-of-plane FWHM for both of the  $Y_2O_3$  buffer layers became narrower than the one for Ni, indicating an improvement in out-of-plane alignment. The in-plane FWHM for the buffer layer is almost the same as that of the underlying Ni. While the YBCO films deposited by co-evaporation and PLD on  $Y_2O_3$  buffer layers, which were deposited at a lower deposition pressure, have a c-axis orientation, the YBCO films deposited by co-evaporation and PLD on  $Y_2O_3$  buffer layer deposited under a higher pressure have a (103) or an a-axis orientation. The grain size of the a-axis or (103) oriented film by PLD is similar to the  $Y_2O_3$  grain size. The crystal orientation and grain size were affected significantly by the surface roughness. The grains in the (001)YBCO films made by PLD were well connected with low porosity. The good crystallinity and morphology lead us to

expect high  $J_c$  values, once the YBCO growth conditions are optimized. However, we believe these results provide evidence that e-beam deposited  $Y_2O_3$  buffer layers can be optimized for the fabrication of a YBCO superconducting tape. We expect that the  $Y_2O_3$  buffer layer has significant value for coated conductors because of its easy fabrication, small lattice mismatch to YBCO, and high chemical stability.

#### ACKNOWLEDGMENT

We would like to thank Shigeo Sunaga of Techno Service for his help in the  $Y_2O_3$  film preparation and Szu-ya Liao for her help in the measurement of superconducting properties.

#### REFERENCES

- [1] D. Dimos and P. Chaudhari and J. Mannhart, Phys. Rev. B41, pp. 4038-4049, 1990.
- [2] N. Heinig, R. D. Redwing, I Fei Tsu, A. Gurevich, J. E. Nordman, S. E. Babcock and D. C. Larbalestier, Appl. Phys. Lett. 69, pp. 544-579, 1995.
- [3] Y. Iijima, K. Onabe, N. Futaki, N. Tanabe, N. Sadakata, O. Kohno and Y. Ikeno, J. Appl. Phys. 74, pp. 1905-1911, 1993.
- [4] X. D. Wu, S. R. Foltyn, P. Arendt, J. Townsend, C. Adams, I. H. Campbell, P. Tiwari, Y. Coulter and D. E. Peterson, Appl. Phys. Lett. 65, pp. 1961-1963, 1994.
- [5] A. Goyal, D. P. Norton, J. D. Budai, M. Paranthaman, E. D. Specht, D. M. Kroger, D. K. Christen, Q. He, B. Saffian, F. A. List, D. F. Lee, P. M. Martin, C. E. Klabunde, E. Hartfield and V. K. Sikka, Appl. Phys. Lett. 69, pp. 1795-1797, 1996.
- [6] A. Ichinose, A. Kikuchi, K. Tachikawa and S. Akita, Physica C 301, pp. 51-56, 1998.